数理解析研究所講究録
第 804 巻 1992 年 75-90

N-Homoclinic Bifurcations of Piecewise Linear Vector Fields

K.Iori* (庵 勝仁)
E.Yanagida** (柳田 英二)
T.Matsumoto* (松本 隆)

*Department of Electrical Engineering, Waseda University, Tokyo 169, Japan
**Department of The Information Sciences, Tokyo Institute of Thecnology, Tokyo 152, Japan

Abstract

N-homoclinic bifurcations (N>2) are found and studied in a piecewise-linear vector field on $\mathbf{R}^3$.

1. Introduction

Consider a two parameter family of vector fields on $\mathbf{R}^n$;

$$\dot{x} = F(x;\mu)$$

Assume:

(i) $F(0,\mu) = 0, \mu \in \mathbf{R}^2, \mu = (\mu_1, \mu_2) \in \mathbf{R}^2$

(ii) $DF(x,\mu)$ has real eigenvalues $\lambda_1, \lambda_2, \lambda_3$ satisfying

$$Re(\lambda_i) < \lambda_2 < \lambda_1 < 0 < \lambda_3 < Re(\lambda_j)$$

where $Re(\lambda_i)$ indicates the real part of other eigenvalues.

(iii) The dynamics has a homoclinic orbit through the origin $x = 0$ at some μ

Homoclinic doubling bifurcation is the phenomenon schematically drawn in Fig1. Namely, a homoclinic orbit of the simplest type (1-homoclinic) orbit bifurcates into a "double-loop" (2-homoclinic orbit) orbit.

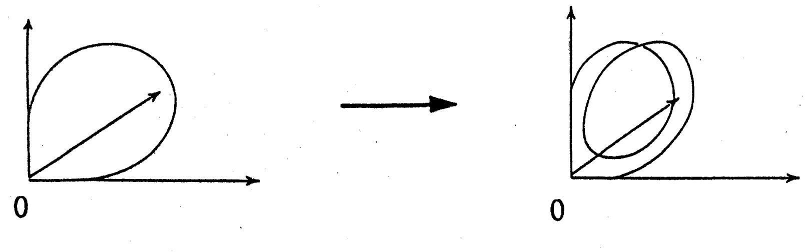

Fig1-1 Simplest homoclinic orbit

Fig1-2."Double-loop" homoclinic orbit

Fig1 Schematic picture of homoclinic doubling bifurcation.

This phenomenon was first found and analyzed by Yanagida [1] during

Fig 2 Critically twisted homoclinic orbit

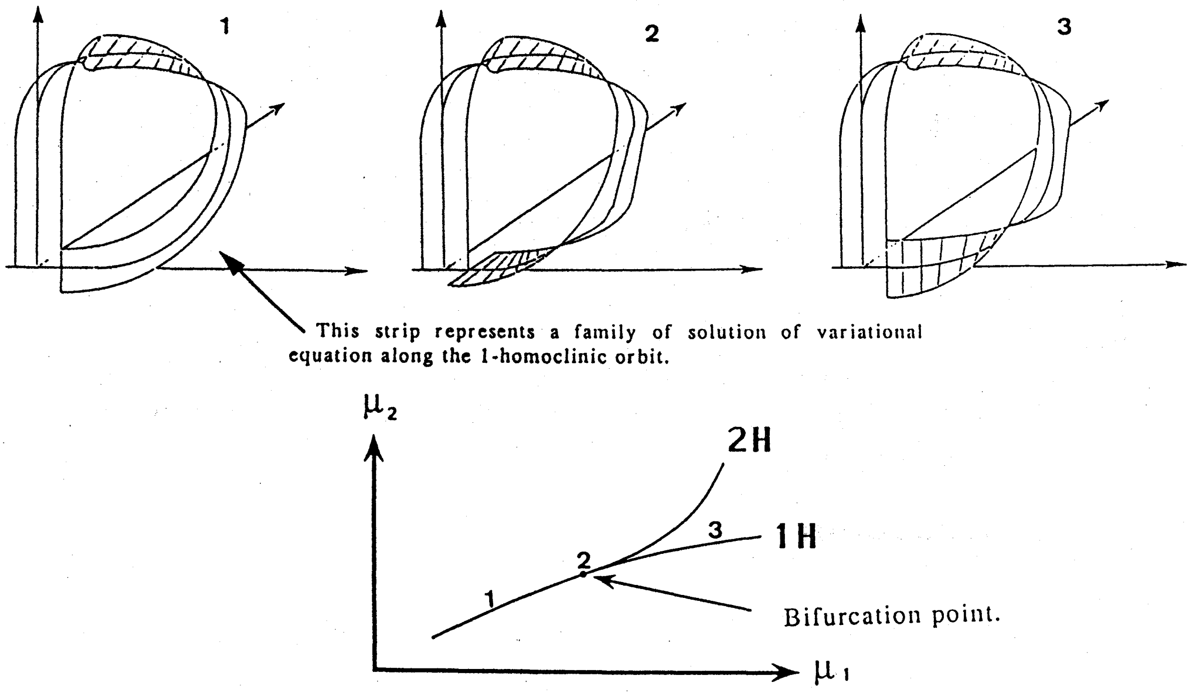

Fig 3 Non - principal homoclinic orbit

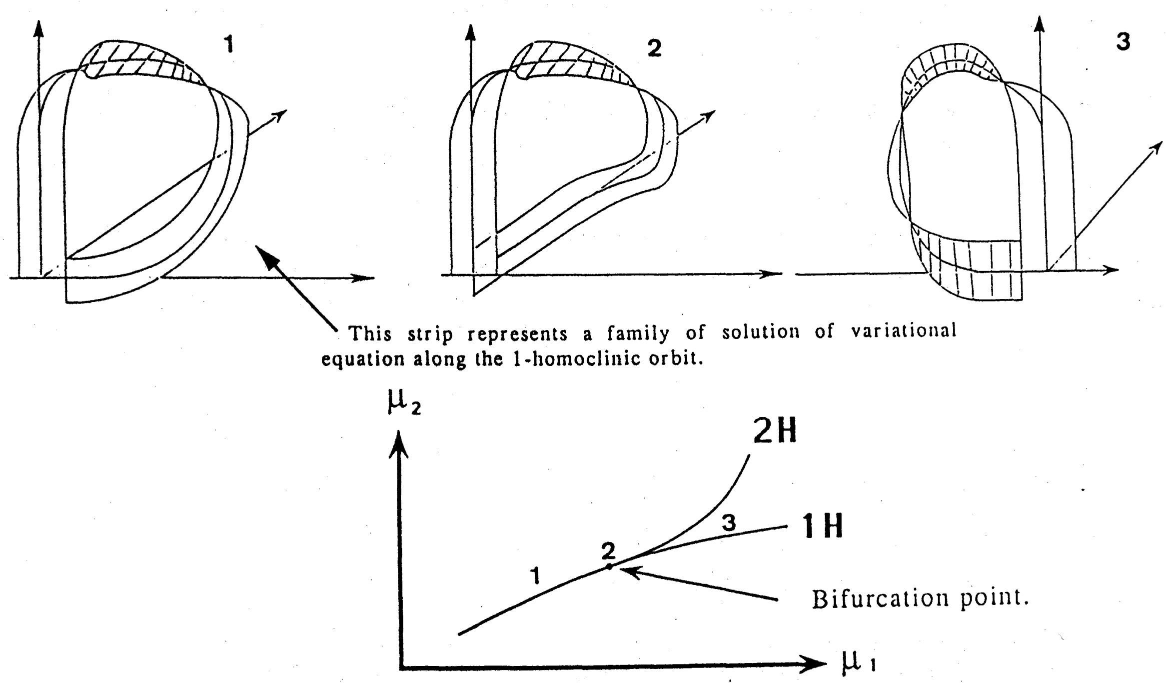

the course of his studies on generalized nerve axon equation. Analyzing with the original partial differential equation, Yanagida derived an ordinary differential equation and proved the existence of a double-pulse traveling wave solution, which corresponds to the homoclinic doubling bifurcation. Yanagida observed that there are three cases in which homoclinic doubling bifurcation can occur:

The original 1-homoclinic orbit is
(1) a homoclinic orbit with *resonant* eigenvalues, or
(2) a *critically twisted* homoclinic orbit, or
(3) a *non-principal* homoclinic orbit.

Case(1) refers to $\lambda_1 + \lambda_3 = 0$ while cases (2) and (3) are schematically shown in Fig2 and Fig3,respectively. M.Kisaka [3] proved that an N(>2)-homoclinic orbit dose not bifurcate from a 1-homoclinic orbit in case (1) and (2). Nothing is known about N(>2)-homoclinic orbits for case(3), however. Details are found in [1],[2],[3],[4]. The purpose of this paper is to give an example which suggests that N(>2)-homoclinic orbit bifurcate from 1-homoclinic orbit for case(3).

2.Normal Forms of 2-Region Continuous Piecewise-Linear Vector Field.

Consider the 2-region continuous piecewise-linear vector field in $\mathbf{R}^3$:

$$\dot{x}' = f(x') = \begin{cases} A'x' & (<\alpha', x'> -1 \le 0) \\ B'x' - p' & (<\alpha', x'> -1 \ge 0) \end{cases} \tag{2.1}$$

where A' and B' are 3x3 matrices and $\mathbf{p}' \in \mathbf{R}^3$. The plane $<\alpha', \mathbf{x}'> = 1$ is the boundary of the vector field. Assume that A' has 3 real eigenvalues λ_1, λ_2, λ_3 ($\lambda_3 > 0 > \lambda_1 > \lambda_2$) and B' has a pair of complex conjugate eigenvalues $\sigma_1 + i\omega_1$ and a real eigenvalue γ_1. ($\sigma_1 < 0, \omega_1 > 0, \gamma_1 > 0$). According to the normal form theorem [5],[6], f is uniquely determined up to linearly conjugacy as follows (provided that f has no eigenspace parallel to the boundary);

$$\boxed{\begin{aligned} \dot{x}'' &= S_A x'' + \frac{1}{2} p'' \{ |<\alpha'', x''> -1| + (<\alpha'', x''> -1) \} \\ &= \begin{cases} S_A x'' & (x'' \in R_-) \\ S_B (x'' - P'') & (x'' \in R_+) \end{cases} \end{aligned} \quad (2.2)}$$

where

$$R_{\pm} = \left\{ \mathbf{x}'' \in \mathbf{R}^3 : \pm(<\alpha'', \mathbf{x}''> -1) > 0 \right\}, \quad \alpha'' =^{T} (1,0,0)$$

$$\mathbf{p}'' =^{T} (c_1, c_2, c_3)$$

$$\mathbf{P}'' =^{T} \left(1 - \frac{a_3}{b_3}, \frac{c_1 a_3}{b_3}, \frac{c_2 a_3}{b_3}\right)$$

$$S_A = \begin{bmatrix} 0 & 1 & 0 \\ 0 & 0 & 1 \\ a_3 & a_2 & a_1 \end{bmatrix}$$

$$S_B = \begin{bmatrix} c_1 & 1 & 0 \\ c_2 & 0 & 1 \\ c_3 + a_3 & a_2 & a_1 \end{bmatrix} = S_A + \mathbf{p}''^{T} \alpha''$$

$$a_1 = \lambda_1 + \lambda_2 + \lambda_3, \; a_2 = -(\lambda_1\lambda_2 + \lambda_2\lambda_3 + \lambda_3\lambda_1), \; a_3 = \lambda_1\lambda_2\lambda_3$$

$$b_1 = 2\sigma_1 + \gamma_1, \; b_2 = -(\sigma_1^2 + \omega_1^2 + 2\gamma_1\sigma_1), \; b_3 = (\sigma_1^2 + \omega_1^2)\gamma_1$$

$$c_1 = b_1 - a_1, \; c_2 = b_2 - a_2 + c_1 a_1, \; c_3 = b_3 - a_3 + c_1 a_2 + c_2 a_1$$

Fig.4 shows the geometric structure of (2.2). The vector field defined by (2.2) is transformed via

$$\mathbf{x}'' = H_A \mathbf{x} \tag{2.3}$$

where

$$H_A = \begin{bmatrix} 1 & 1 & 1 \\ \lambda_1 & \lambda_2 & \lambda_3 \\ \lambda_1^2 & \lambda_2^2 & \lambda_3^2 \end{bmatrix}$$

to the vector field

$$\boxed{\begin{aligned} \dot{\mathbf{x}} &= A\mathbf{x} + \frac{1}{2}\mathbf{p}\{|<\alpha, \mathbf{x}> -1| + (<\alpha, \mathbf{x}> -1)\} \\ &= \begin{cases} A\mathbf{x} & (\mathbf{x} \in R_-) \\ B(\mathbf{x} - \mathbf{p}) & (\mathbf{x} \in R_+) \end{cases} \end{aligned} \qquad (2.4)}$$

where

$$A = \begin{bmatrix} \lambda_1 & 0 & 0 \\ 0 & \lambda_2 & 0 \\ 0 & 0 & \lambda_3 \end{bmatrix}$$

$$\alpha = {}^{T}(1,1,1) \qquad p = H_A^{-1}p'' \qquad P = B^{-1}p$$
$$B = A + p^{T}\alpha$$
$$R_{\pm} = \{x \in R^3 : \pm(<\alpha, x> -1) > 0\}$$
$$V = \{x \in R^3 : <\alpha, x> = 1\}$$
$$V_{-} = \{x \in V : {}^{T}\alpha A x < 0\}$$
$$V_{+} = \{x \in V : {}^{T}\alpha A x > 0\}$$

This is called the *normal form* of 2-region continuous piecewise-linear vector field.
Fig5. shows the geometric structure of (2.4).

3.Bifurcation equations.

3.1 Return time coordinate.

Consider a point $\tilde{x}$ lying on the boundary V. Let $\tilde{y}$ and $\tilde{z}$ be the points at which the trajectory starting from $\tilde{x}$ hits V again at positive time s and negative time -t ,respectivry. Since the system is linear in each region, one has

$$\tilde{y} = e^{Bs}(\tilde{x} - P) + P \qquad (3.1.1)$$
$$\tilde{z} = e^{-At}\tilde{x} \qquad (3.1.2)$$

Since the vector field is continuous ,

$$A\tilde{x} = B(\tilde{x} - P) \qquad \tilde{x} \in V \qquad (3.1.3)$$
$$A\tilde{y} = B(\tilde{y} - P) \qquad \tilde{y} \in V \qquad (3.1.4)$$

Using (3.1.4) and (3.1.1), one has

$$A\tilde{y} = Be^{Bs}(\tilde{x} - P)$$

Since A is non-singular,

$$\tilde{y} = A^{-1}e^{Bs}B(\tilde{x} - P) \qquad (3.1.5)$$

Moreover, by (3.1.3), one has

$$\tilde{y} = A^{-1}e^{Bs}A\tilde{x} = e^{Cs}\tilde{x}$$

where

$$C = A^{-1}BA$$

Since $\tilde{x}, \tilde{y}$ and $\tilde{z}$ are on the boundary V

$${}^{T}\alpha e^{-At}\tilde{x} = 1 \qquad {}^{T}\alpha\tilde{x} = 1 \qquad {}^{T}\alpha e^{Cs}\tilde{x} = 1$$

so that

$$\left[e_1{}^{T}\alpha e^{-At} + e_2{}^{T}\alpha + e_3{}^{T}\alpha e^{Cs}\right]\tilde{x} = h \qquad (3.1.6)$$

where

$$e_1 = {}^{T}(1,0,0)\ ,\ e_2 = {}^{T}(0,1,0)\ e_3 = {}^{T}(0,0,1)\ ,\ h = {}^{T}(1,1,1)$$

If

$$K(s,t) = \left[e_1{}^{T}\alpha e^{-At} + e_2{}^{T}\alpha + e_3{}^{T}\alpha e^{Cs}\right]^{-1} \qquad (3.1.7)$$

is non singular, then

$$\tilde{x} = K(s,t)\mathbf{h} \qquad (3.1.8)$$

The pair (s,t) is called the *return time coordinate* of $\tilde{x}$ on V. (See Fig6. and Fig7).

3.2 Homoclinic bifurcation equations.

If a trajectory starting from (0,1,1) hits $E^C(0)$ on the boundary V, then it is a 1-homoclinic orbit through the origin (Fig4.) which is chracterised by

$$\boxed{\begin{aligned} &{}^T\alpha e^{Cs}e_3 - 1 = 0 \\ &{}^T e_3 e^{Cs} e_3 = 0 \end{aligned} \qquad (3.2.1)}$$

Fig8. shows a 1-homoclinic orbit. Similarly, an N-homoclinic orbit through the origin is characterized by

$$\boxed{\begin{aligned} &{}^T\alpha e^{Cs_1}e_3 - 1 = 0 \\ &N(e^{Cs_1}e_3 - e^{-At_2}K(s_2,t_2)\mathbf{h}) = 0 \\ &N(e^{Cs_i}K(s_i,t_i)\mathbf{h} - e^{-At_{i+1}}K(s_{i+1},t_{i+1})\mathbf{h}) = 0 \\ &(2 \le i \le m-1) \\ &{}^T e_3 e^{Cs_m}K(s_m,t_m)\mathbf{h} = 0 \end{aligned} \qquad (3.2.2)}$$

where

$$N = \begin{bmatrix} 1 & 0 & 0 \\ 0 & 1 & 0 \end{bmatrix}$$

Fig9 shows a typical 3-homoclinic orbit.

3.3 Tangent map

Assume that there exists an s_0 such that

$$z_0 = e^{Bs_0}(y_0 - \mathbf{P}) + \mathbf{P} \qquad (y_0 \in V_+, z_0 \in V_-),$$

$${}^T\alpha\{e^{Bs}(y_0 - \mathbf{P}) + \mathbf{P}\} - 1 \neq 0 \quad , \quad {}^\forall s \in (0, s_0)$$

Let

$$H(y,s) = {}^T\alpha\{(e^{Bs}(y - \mathbf{P})) + \mathbf{P}\} - 1$$

Since

$$H(y_0, s_0) = {}^T\alpha z_0 - 1 = 0,$$

and since

$$\frac{\partial H}{\partial t}(y_0, s_0) = {}^T\alpha B e^{Bs_0}(y_0 - \mathbf{P}) = {}^T\alpha B(z_0 - \mathbf{P}) = {}^T\alpha A z_0 \neq 0$$

there exist a neighborhood $V_+(y_0)$ of y_0 on V_+ and function (called a return time function)

$$s: V_+(y_0) \to \mathbf{R}$$

such that

$$H(y,s(y))=0,\ s(y_0)=s_0,$$

Then,

$$Ds(y_0)=-\left[\frac{\partial H}{\partial t}(y_0,s_0)\right]^{-1}\cdot\frac{\partial H}{\partial y}(y_0,s_0)$$

$$=-\left[{}^{T}\alpha A z_0\right]^{-1}{}^{T}\alpha e^{Bs_0}$$

Let

$$g(y)=e^{Bs(y)}(y-p)+p.$$

Then one can show that the tangent map is given by,

$$\boxed{\begin{aligned} Dg(y_0)&=Be^{Bs_0}(y_0-\mathbf{P})Ds(y_0)+e^{Bs_0}\\ &=B(z_0-\mathbf{P})Ds(y_0)+e^{Bs_0}\\ &=\left\{I-\frac{Az_0{}^{T}\alpha}{{}^{T}\alpha Az_0}\right\}e^{Bs_0} \qquad (3.3.1)\end{aligned}}$$

3.4 Conditions for homoclinic doubling bifurcation.

Define(See Fig10)

$$\boxed{\begin{aligned} &h_1(\lambda_1,\lambda_2,\lambda_3,\sigma_1,\omega_1,\gamma_1)={}^{T}e_1e^{Bs_0}e_3\\ &\qquad\qquad (3.4.1)\\ &h_2(\lambda_1,\lambda_2,\lambda_3,\sigma_1,\omega_1,\gamma_1)={}^{T}e_3\left\{I-\frac{Az_0{}^{T}\alpha}{{}^{T}\alpha Az_0}\right\}e^{Bs_0}(e_1-e_3)\end{aligned}}$$

Then, a homoclinic doubling bifurcation is characterized by

(1) homoclinic orbit with resonant eigenvalues;

$$h_1(\lambda_1,\lambda_2,\lambda_3,\sigma_1,\omega_1,\gamma_1)\times h_2(\lambda_1,\lambda_2,\lambda_3,\sigma_1,\omega_1,\gamma_1)<0$$

and (3.4.2)

$$|\lambda_1|=|\lambda_3|$$

(2) critically twisted homoclinic orbit;

$$h_2(\lambda_1,\lambda_2,\lambda_3,\sigma_1,\omega_1,\gamma_1)=0$$

and (3.4.3)

$$|\lambda_1|<|\lambda_3|$$

(3) non-principal homoclinic orbit;

$$h_1(\lambda_1,\lambda_2,\lambda_3,\sigma_1,\omega_1,\gamma_1)=0$$

and (3.4.4)

$$|\lambda_1|<|\lambda_3|$$

4. Bifurcation sets of N-homoclinic orbits.

4.1 Two parameter diagram.

Fig11 shows N-homoclinic bifurcation sets,for N=1~7, in the (λ_1,σ_1)-space obtained by solving (3.2.1) and (3.2.2). The vertical axis is σ_1 while the horizontal axis is λ_1. The other eigenvalues are fixed as

$$\omega_1 = 1.0 \ , \ \gamma_1 = -0.01 \ , \ \lambda_2 = -0.32 \ , \ \lambda_3 = 0.3 \qquad (4.1.1)$$

Fig12 shows details of Fig11 where bifurcation sets for N=8 and 9 are discernible. Fig13 shows the same bifurcation sets in the range $-0.8<\lambda_1<-0.4$, whereas Fig14 shows details of Fig13. NH in these figures indicates N-homoclinic bifurcation sets. For N=3 and 5~9,homoclinic bifurcation sets form a loop while 4-homoclinic bifurcation sets consist of two loops. Moreover, it appears that all the N(3~9)-homoclinic bifurcation sets bifurcate from a point on the 1-homoclinic bifurcation set. Fig15 shows the orbits corresponding to the bifurcation sets. For 1H in Fig15, the numbers 1,2 and 3 correspond to those in Fig3.

4.2 Non-principal homoclinic orbit.

Solving the set of Eqs.(3.2.1) and (3.4.4) by Newton method,we obtained the following set of values:

$$\sigma_1 = 0.0137 \ , \ \lambda_1 = -0.01$$

These are the values on which non-principal homoclinic orbit exists. Now let us look at this point in Fig12. It appears that all the N(>2)-homoclinic bifurcation sets accumulate towards this point.This phenomenon suggests that there is a close relationship between N(>2)-homoclinic orbits and non-principal homoclinic orbit.

4.3 Three dimensional bifurcation diagram.

Fig16 shows a three dimensional bifurcation diagram of 3-homoclinic bifurcation set. Here γ_1 is fixed as $\gamma_1=-0.04$ while others are the same as in (4.1.1). This figure shows that 3-homoclinic bifurcation sets vanish if λ_2 is sufficiently larger than -0.3. Kisaka [3] proved under several conditions of eigenvalues including the case $|\lambda_2| > |\lambda_3|$ that N(>2)-homoclinic orbit *dose not* bifurcate from 1-homoclinic orbit for the critically twisted case. This, however, dose not contradict our numerical results because for the latter, Kisaka's conditions are not satisfied.

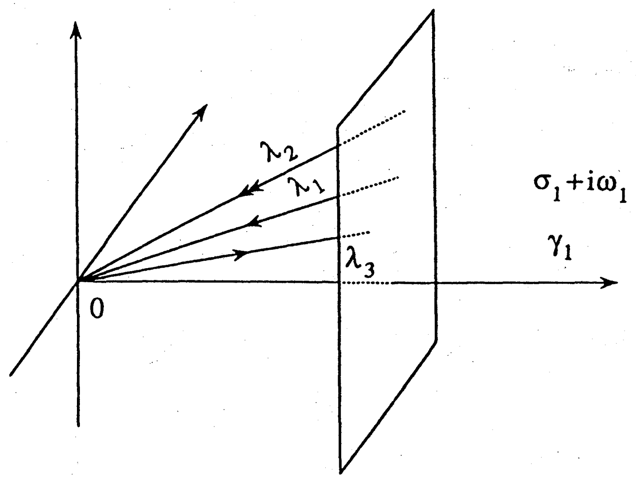

Fig 4 Geometric structure of (2.2).

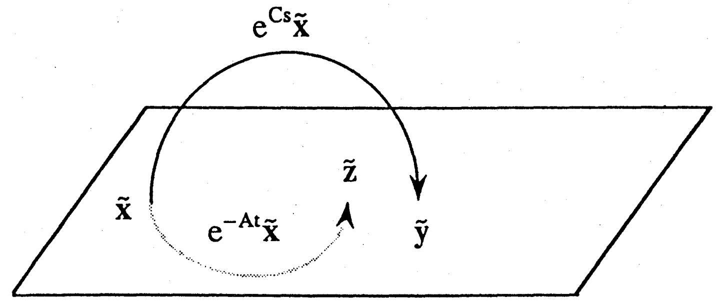

Fig 6 Poincare half return map.

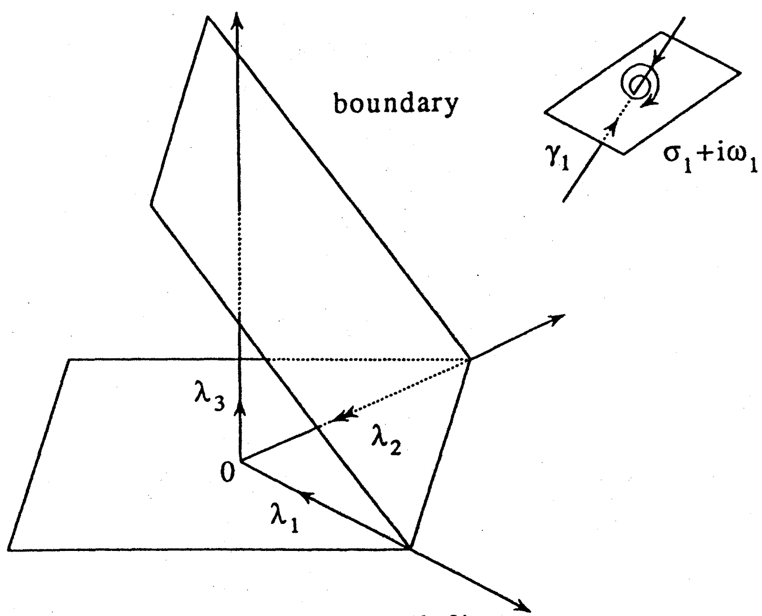

Fig 5 Geometric structure of (2.3).

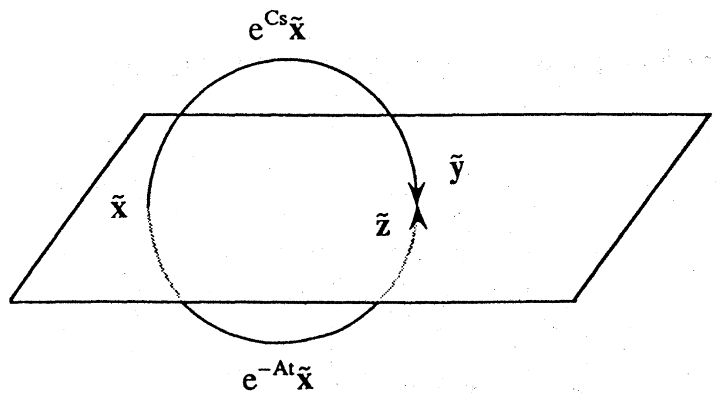

Fig 7 Poincare full return map.

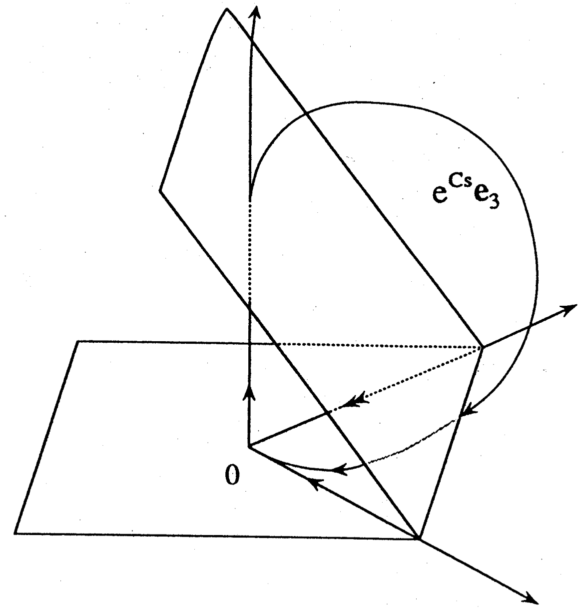

Fig 8 1-homoclinic orbit.

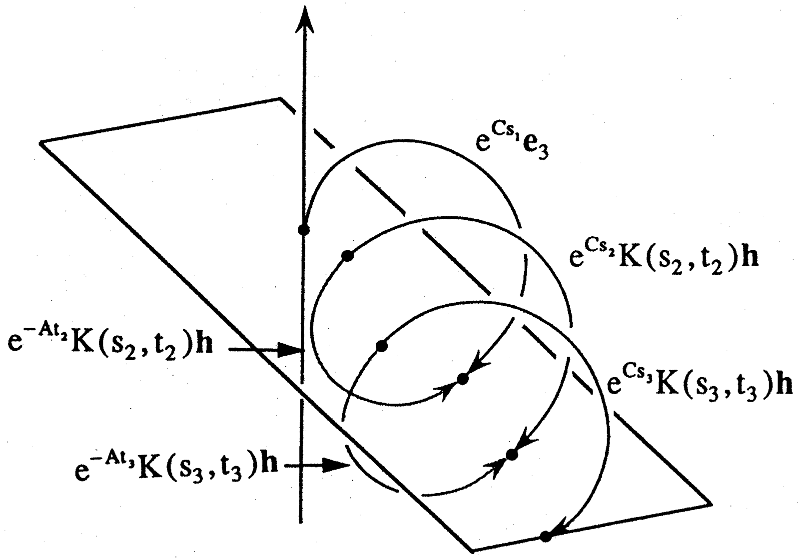

Fig 9 3-homoclinic orbit.

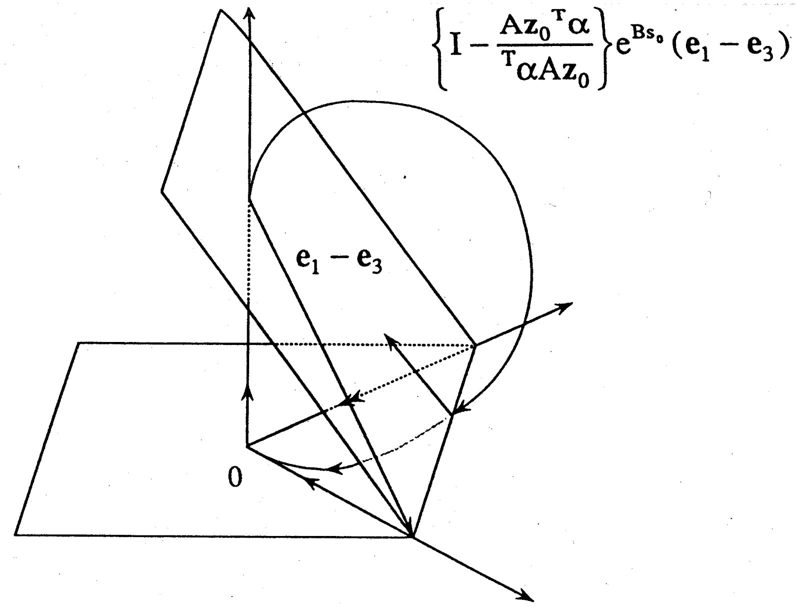

Fig 10 Conditions for homoclinic doubling bifurcation.

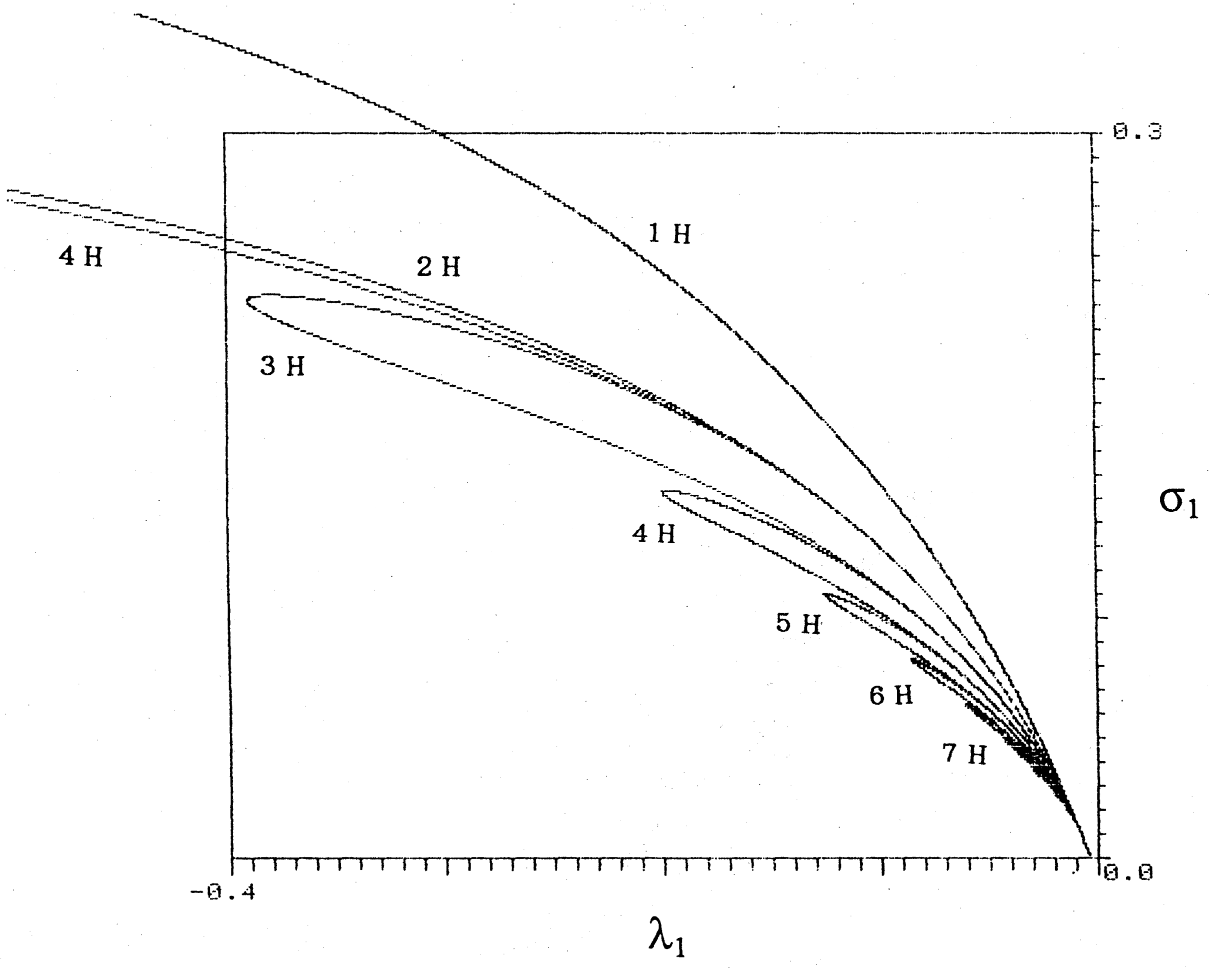

Fig 11 Two parameter bifurcation diagram.
N(1~7)-homoclinic bifurcation set.

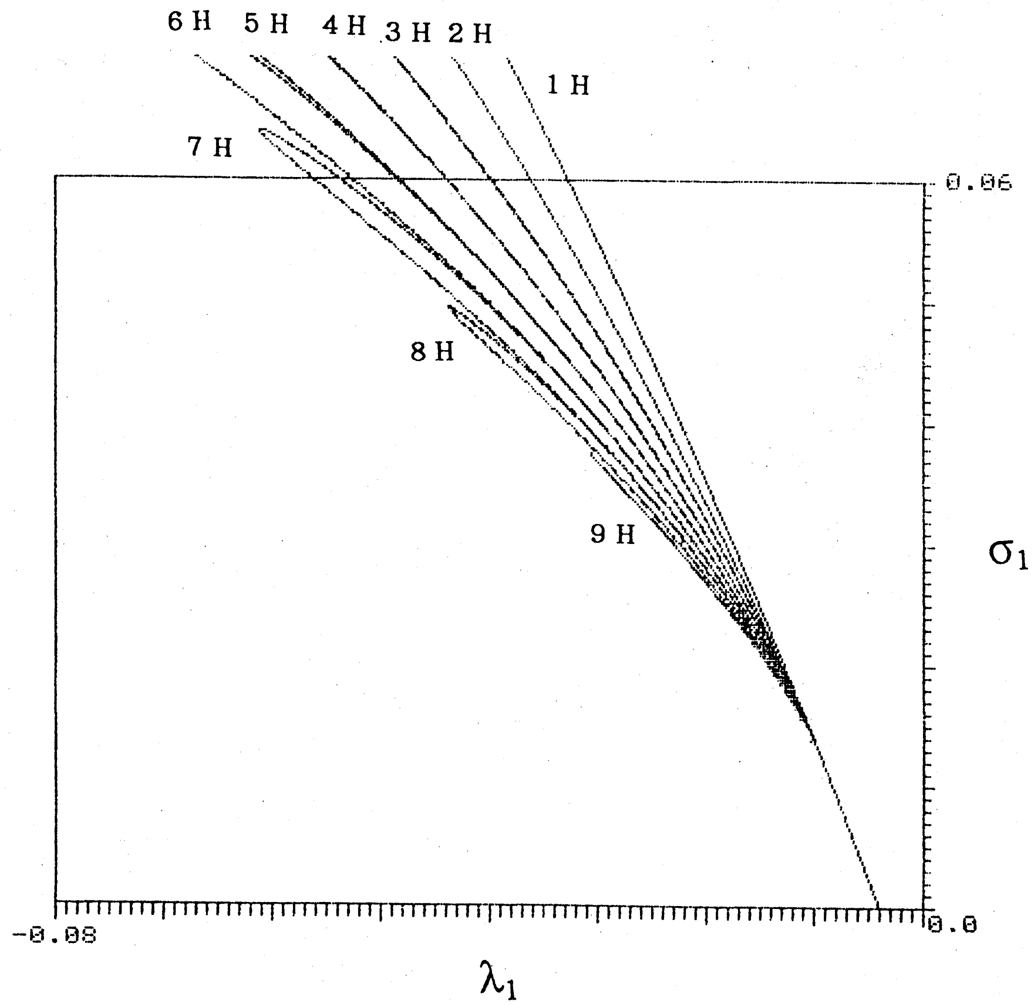

Fig 12 Detailes of Fig 11.

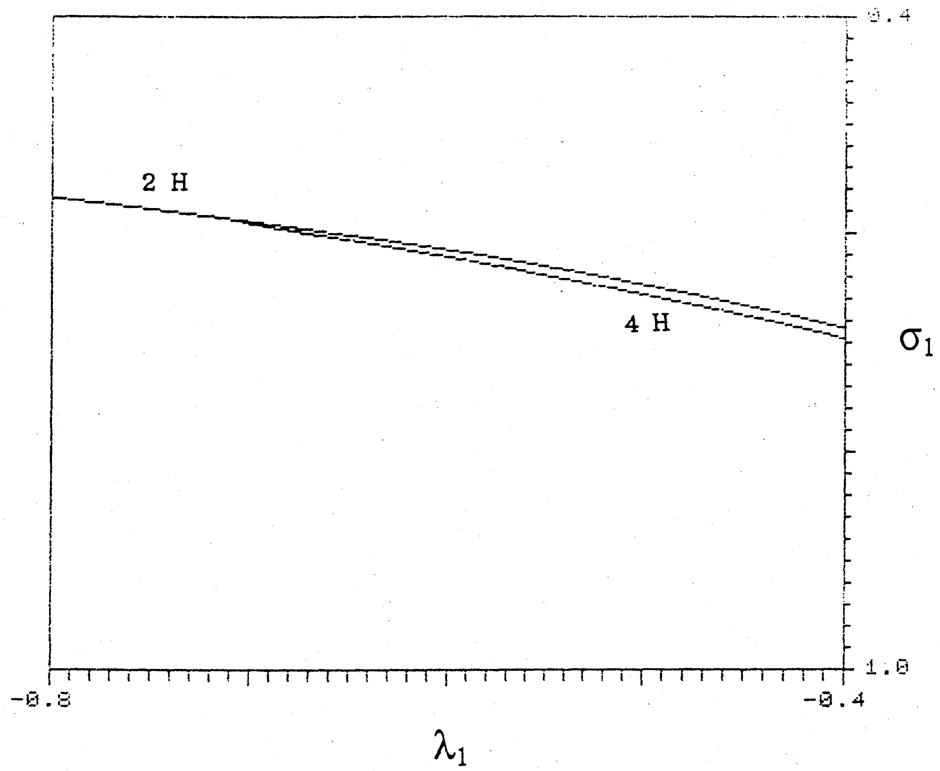

Fig 13 Two parameter bifurcation diagram.

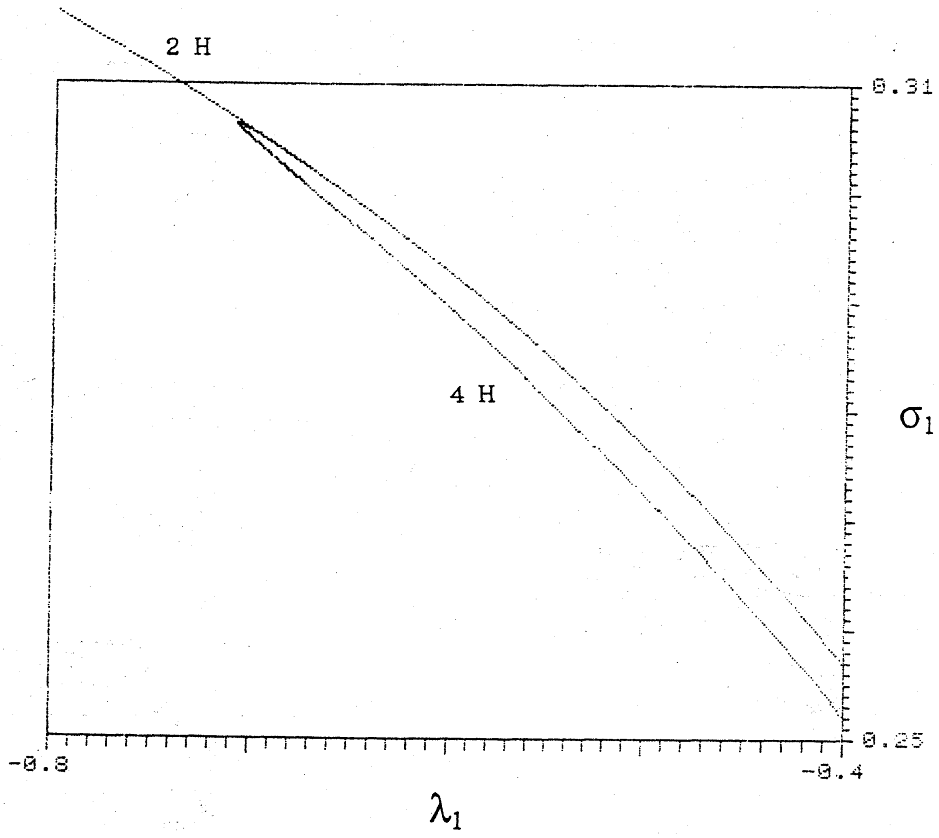

Fig 14 Detailes of Fig 13.

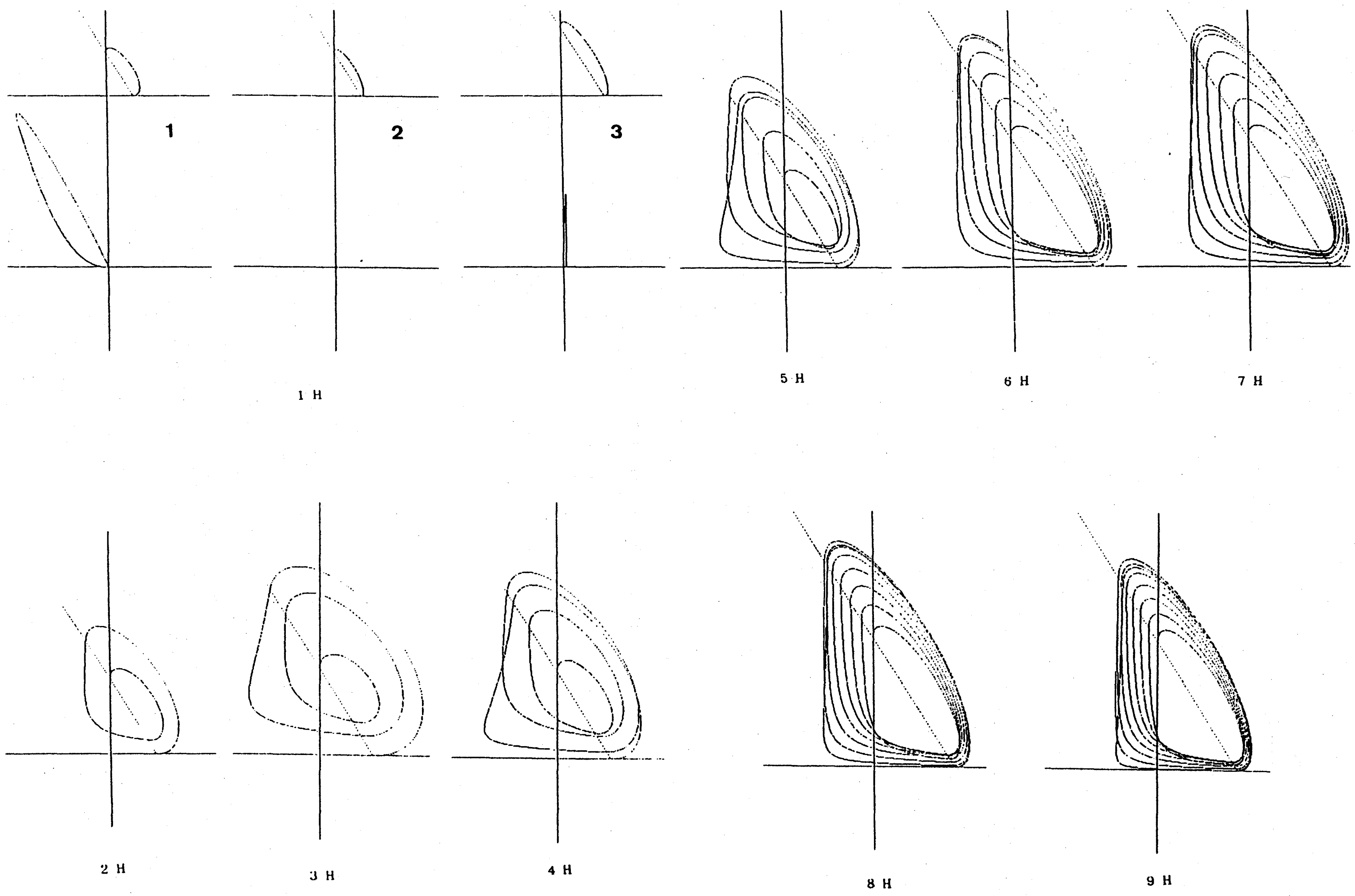

Fig 15 N(1~9)-homoclinic orbit.

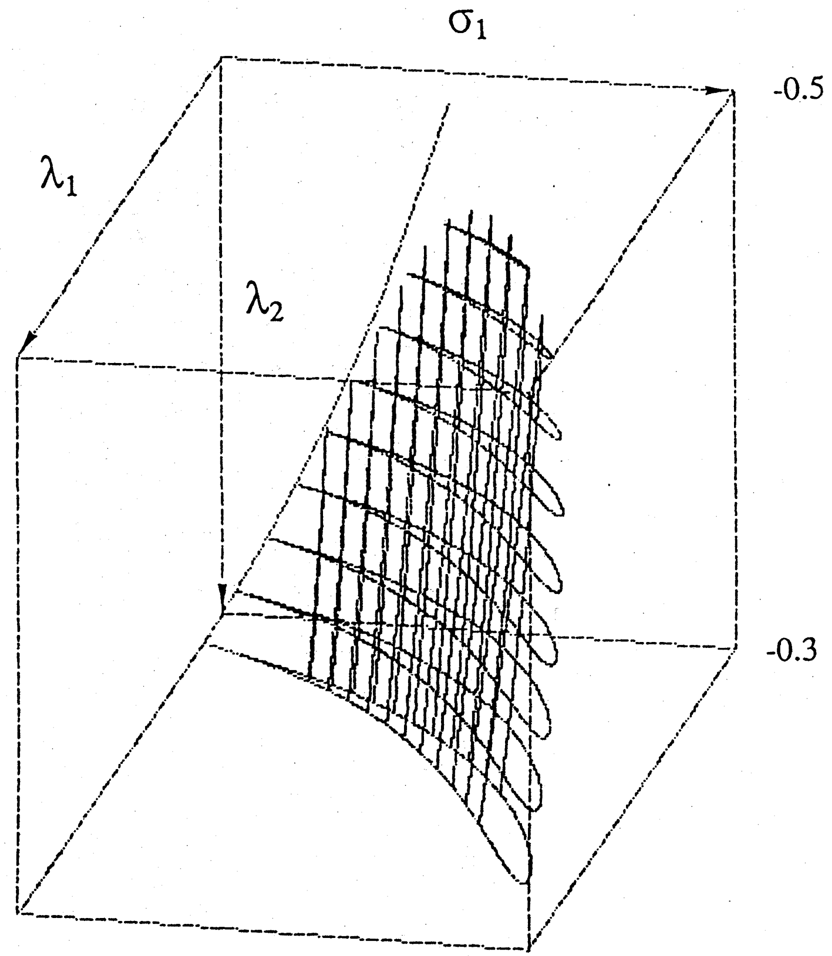

Fig 16 Three dimensional bifurcation diagram.
3-homoclinic orbit.

Acknowledgments.

We would like to thank M.Komuro of Nishi-Tokyo University, H.Kokubu, M.Kisaka of.Kyoto University, R.Tokunaga of Tukuba University,Y.Abe and K.Tanaka of Waseda University for their constructive comments.

References.

[1]E.Yanagida,"Branching of double pulse solutions from single pulse solutions in nerve axon equations.",J.Diff.Eqs.66(1987),243-262.

[2]H.Kokubu,"Homoclinic and Heteroclinic bifurcations of vector fields.",Jap.J.Appl.Math.5(1988),455-501.

[3]M.Kisaka,H.Kokubu,and H.Oka, in preparation; M.Kisaka, master thesis,1991,Kyoto University(in Japanese).

[4]S.-N.Chow,B.Deng,and B.Fiedler,"Homoclinic bifurcation at resonant eigenvalues.",J.Dyn.Diff.Eqs.2(1990),177-244.

[5]M.Komuro,"Normal forms of continuous piecewise linear vector fields and chaotic attractors.Part 1.",Jap.J.Math.5(1988),257-304.

[6]M.Komuro,"Normal forms of continuous piecewise linear vector fields and chaotic attractors.Part 2.",Jap.J.Math.5(1988),503-549.

[7]M.Komuro,"Bifurcation equations of continuous piecewise linear vector fields.",Jap.J.Appl.Math. to appear.